Precision lifetime measurements of a single trapped ion with ultrafast laser pulses

D. L. Moehring,* B. B. Blinov, D. W. Gidley, R. N. Kohn, Jr., M. J. Madsen, T. D. Sanderson, R. S. Vallery, and C. Monroe
FOCUS Center and Department of Physics, University of Michigan, Ann Arbor, Michigan 48109-1040, USA
(Received 15 May 2005; published 14 February 2006)

We report precision measurements of the excited state lifetime of the $5p\ ^2P_{1/2}$ and $5p\ ^2P_{3/2}$ levels of a single trapped Cd^+ ion. Combining ion trap and ultrafast laser technologies, the ion is excited with picosecond laser pulses from a mode-locked laser and the distribution of arrival times of spontaneously emitted photons is recorded. The resulting lifetimes are 3.148 ± 0.011 ns and 2.647 ± 0.010 ns for $^2P_{1/2}$ and $^2P_{3/2}$ respectively. With a total uncertainty of under 0.4%, these are among the most precise measurements of any atomic state lifetimes to date.

DOI: 10.1103/PhysRevA.73.023413 PACS number(s): 32.80.Pj, 32.70.Cs, 42.50.Vk

Precise measurements of atomic data are of great interest throughout many fields of science. Lifetime measurements are of particular importance to the interpretation of measurements of atomic parity nonconservation [1], tests of QED and atomic structure theory [2], and even astrophysical applications [3]. Because of this, new and more accurate ways of measuring excited state lifetimes are constantly being investigated. Previous methods include time-correlated single photon techniques [4–9], beam-foil experiments [5], fast beam measurements [10,11], electron-photon delayed coincidence techniques [12,13], luminescent decay [14,15], linewidth measurements [16], photoassociative spectroscopy [17], and quantum jump methods [18].

Here we report excited state lifetime measurements using a time-correlated single photon-counting technique. The experiment uniquely combines the isolation of single laser-cooled trapped ions with the precise timing of ultrafast lasers. This method, designed especially to eliminate common systematic errors, involves selective excitation of a single trapped ion to a particular excited state (lifetime of order nanoseconds) by an ultrafast laser pulse (duration of order picoseconds). Arrival of the spontaneously emitted photon from the ion is correlated in time with the excitation pulse, and the excited state lifetime is extracted from the distribution of time delays from many such events.

By performing the experiment on a single trapped ion [6,7,18], we are able to eliminate prevalent systematic errors, such as pulse pileup that causes multiple photons to be collected within the time resolution of the detector, radiation trapping or the absorption and re-emission of radiation by neighboring atoms, atoms disappearing from view before decaying, and subradiance or superradiance arising from coherent interactions with nearby atoms. By using ultrafast laser pulses [4], we can eliminate potential effects from applied light during the measurement interval including ac Stark shifts, background laser light, and multiple excitations which can also lead to pulse pileup.

With this setup, at most one photon can be emitted following an excitation pulse. While this feature is instrumental in eliminating the above systematic errors, it would appear that this signal would require large integration times for reasonable statistical uncertainties. However, with a lifetime of only a few nanoseconds, millions of such excitations can be performed each second, thus potentially allowing sufficient data for a statistical error of under 0.1% to be collected in a matter of minutes [6].

A diagram of the experimental apparatus is shown in Fig. 1. Individual cadmium ions are trapped and isolated in one of two rf quadrupole traps. First, the experiment is conducted using an asymmetric quadrupole trap of characteristic size ~ 0.7 mm [19] [Fig. 1(c)]. The entire experiment is then repeated in a linear trap with rod spacings of 0.5 mm and an endcap spacing of 2.6 mm [Fig. 1(d)]. Both traps have secular trapping frequencies on the order of $\omega/2\pi \sim 0.1-1.0$ MHz.

Two types of laser radiation are incident on the ion: pulsed and continuous wave (cw) lasers. The pulsed light is from a picosecond mode-locked Ti:sapphire laser whose center frequency is resonantly tuned to provide excitation to one of the ^2P states [Fig. 1(b)]. For excitation to the $5p\ ^2P_{1/2}$ ($5p\ ^2P_{3/2}$) state, each pulse is frequency quadrupled from 906 to 226.5 nm (858 to 214.5 nm) through phase-matched LBO and BBO nonlinear crystals. The UV is filtered from the fundamental and second harmonic via dichroic mirrors and directed to the ion with a near transform-limited pulse width of $t_{\mathrm{uv}} \approx 1$ ps. Since the pulsed laser bandwidth (~ 0.40 THz) is much smaller than the fine-structure splitting (~ 74 THz), selective excitation to the different ^2P excited states is possible. Each pulse has $E \approx 10$ pJ of energy, which will excite the ion with a probability of approximately 10% [20]: $P_{exc} = \sin^2\sqrt{(\gamma^2/4\pi I_s)(E t_{\mathrm{uv}}/w_o^2)}$, where γ is the atomic linewidth, I_s is the saturation intensity, and $w_o \approx 6$ μm is the beam waist. This pulsed laser is also used to load ions in the trap via photoionization by tuning to the neutral cadmium $^1S_0$-$^1P_1$ resonance at 228.8 nm. Once loaded, a single ion will typically remain in the trap for several days.

After the ion is loaded, it is crystallized within the trap via Doppler cooling on the $D2$ line at 214.5 nm using the cw laser. This laser is tuned approximately one linewidth to the red of resonance and localizes the ion to under 1 μm. Residual micromotion at the rf drive frequency (~ 40 MHz) is reduced via offset electric fields supplied from compensation electrodes [21]. We estimate the kinetic energy from this micromotion to be under 1 K.

*Electronic address: dmoehrin@umich.edu

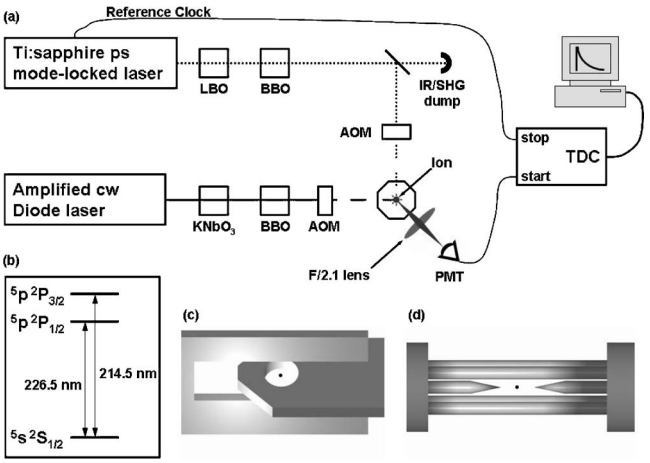

FIG. 1. The experimental apparatus. (a) A picosecond mode-locked Ti:sapphire laser is tuned to four times the resonant wavelength for either the $5p\ ^2P_{1/2}$ or the $5p\ ^2P_{3/2}$ level of Cd^+. Each pulse is then frequency-quadrupled through nonlinear crystals, filtered from the fundamental and second harmonics, and directed to the ion. An amplified cw diode laser is also frequency quadrupled and tuned just red of the $^2P_{3/2}$ transition for Doppler cooling of the ion within the trap. Acousto-optic modulators (AOM) are used to switch on and off the lasers as described in the text. Photons emitted from the ion are collected by an $f/2.1$ imaging lens and directed toward a photon-counting photomultiplier tube (PMT). The output of the PMT provides the start pulse for the time to digital converter (TDC), whereas the stop pulse is provided by the reference clock of the mode-locked laser. (b) The relevant energy levels of Cd^+. (c) An asymmetric quadrupole trap. (d) A linear trap.

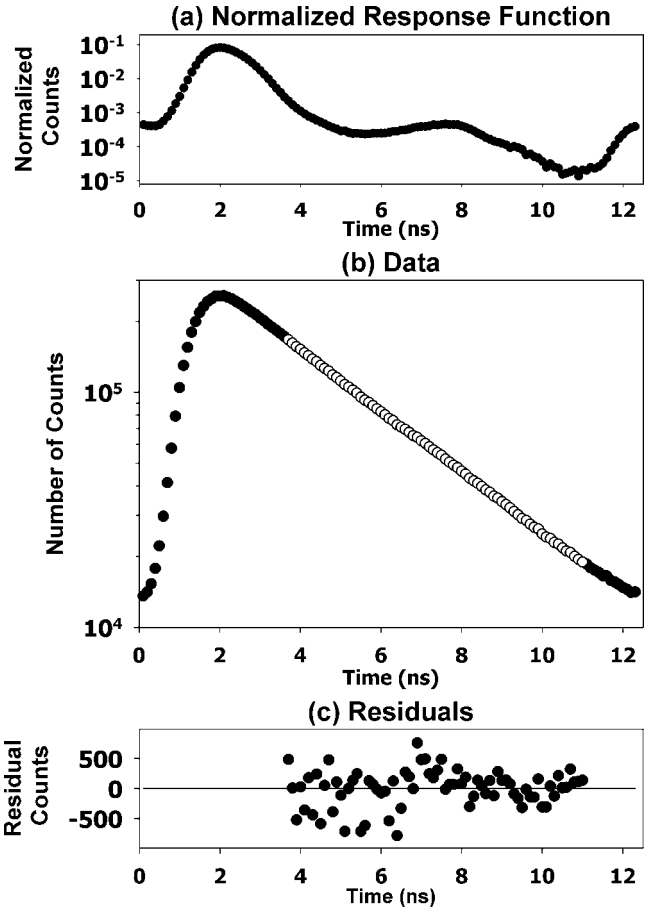

FIG. 2. (a) The response function of the instrument when viewing light scattered off an electrode surface (no atomic physics). The main peak asymmetry is due to the response time of the PMT of ≈0.5 ns, whereas the secondary peaks are due to noise in the TDC triggering electronics (~0.6% of the main peak amplitude). While laser light scattered off an electrode is not a single photon source, this curve was taken at a sufficiently low photon collection rate so that pulse pileup effects were negligible. (b) Data for the $5p\ ^2P_{1/2}$ state taken in the quadrupole trap. The open circles show the data used to extract the excited state lifetime (see text). (c) The deviations from the fit function (residuals). Due to the difficulty in accurately defining a prompt peak background, the fit is not performed around the time of the excitation pulse. This has a small effect on the residuals, but as discussed in the text, is virtually independent of the resulting extracted lifetime.

Following excitation from the pulsed laser, the spontaneously emitted photons are collected by an $f/2.1$ imaging lens and directed toward a photon-counting photomultiplier tube (PMT) [22]. The output signal of the PMT provides the start pulse for the time-to-digital converter (TDC), whereas the stop pulse is synchronized to the reference clock of the mode-locked laser. This time-reversed mode is used to eliminate dead time in the TDC. The PMT used is a Hamamatsu H6240 Series PMT of quantum efficiency ≈20%, and the TDC is an ORTEC model 9353 time digitizer that has 100 ps digital time resolution with no interpolator, accuracy within 20 ppm, less than 145 ps time jitter, and an integral nonlinearity within 20 ps rms.

In the experiment, an acousto-optic modulator (AOM) is used to switch on the cw beam to Doppler cool the ion for 500 ns. Following the cooling pulse, a reference clock from the pulsed laser (synchronized with the laser pulse train) triggers an AOM in the pulsed laser beam and directs a number of pulses to the ion (≈15 pulses, with adjacent pulses separated by ≈12.4 ns). The repetition rate of this cycle is limited to 1 MHz due to the update time of the pulse generator, and during a given excitation pulse the success probability of detecting an emitted photon is $\sim 2\times 10^{-4}$. This gives an average count rate of about 3000 counts per second and thus an expected statistical precision of $\Delta\tau_{rms}/\tau \approx 0.25\%/\sqrt{T}$, where τ is the excited state lifetime and T is the data collection time in minutes.

Despite the absence of previously mentioned common systematic effects, possible effects that still must be considered in this system include Zeeman and hyperfine quantum beats [31]. Zeeman quantum beats have no significant effect (shifts of $<0.05\%$) when working in sufficiently low magnetic fields (<0.5 G), whereas the hyperfine beating is eliminated by using an even isotope of Cd that has no hyperfine structure (i.e., $^{110}Cd^+$). Potential effects from off-resonant laser light—ac stark shifts, background counts, etc.—are also greatly reduced or eliminated in this experiment by taking data only when the cw cooling beam is switched off via the AOM. Hence, immediately following the excitation pulse, the only light present is the single spontaneously emitted photon from the ion. Other possible effects such as relativistic shifts or isotopic dependencies are negligible. Because

TABLE I. Lifetime measurement results (ns). The asymmetric quadrupole and linear trap results are in good statistical agreement for the $^2P_{3/2}$ transition and the final result is a weighted average of the two values (the systematic error is common to both). For the $^2P_{1/2}$ transition, the contribution from the linear trap is omitted from the final result due to an order of magnitude larger prompt peak giving rise to an unusually large systematic error.

Trap	Error	$5p\ ^2P_{1/2}$	$5p\ ^2P_{3/2}$
Quadrupole	…	3.148	2.646
	Statistical	0.005	0.002
	Systematic	0.010	0.010
Linear	…	3.132	2.649
	Statistical	0.002	0.003
	Systematic	0.030	0.010
Final results		3.148±0.011	2.647±0.010

this technique is devoid of these typical systematic effects, the only significant errors are those arising from the particular equipment used, as discussed below.

To determine the excited state lifetime, the data in a 12.4 ns range for each laser pulse are summed and time-inverted. These spectra are corrected for uncorrelated background events and then fit to a single exponential lifetime τ. As the start time of the fit is stepped-out from the peak [32], the fitted lifetime for the experimental data has an expected systematic bias of 3–5 % (a natural consequence of the convolution of the timing system response function [Fig. 2(a)] with the pure exponential decay of the excited state). This effect can be further exacerbated by the presence of "prompt" events from background laser light from the ultrafast excitation pulse that is scattered from the apparatus, described by an additional convolution of a δ function at $t=0$. The relative intensity of the prompt peak varies between the four measurements, and depends upon the particular optical alignment in each experimental run. The time-response function distorts the spectrum from a pure exponential and has the net effect of shifting events to longer times thereby increasing the fitted lifetime by 3–5 %. To account for these time-dependent shifts and extract the true lifetime, a simulated spectrum is generated by convolving the measured time-response function with an exponential decay and δ function at $t=0$. The relative intensity of the prompt δ function is straightforwardly determined by subtracting a convolved pure exponential, appropriately normalized in the exponential part of the spectrum, and integrating the remaining events around $t=0$.

The simulated spectra and the real data are fit in precisely the same manner: the start channel of the fit is successively stepped out from $t_s=1$ ns to $t_s=6$ ns. The parameter τ in the simulated spectra is varied to best match the fitted data over the entire time range. The systematic error in the lifetime is determined by varying τ until the data over the time range is no longer in statistical agreement with the simulated spectra. While the resulting variation of the fits over the full fitting range for the simulations are sensitive to the choice of the prompt δ-function intensity, the fitted lifetime over the range $t_s=1.7$–1.8 ns is virtually independent of the prompt δ-function intensity and thus the results for the lifetimes and the statistical error bar quoted in Table I are taken from this range of t_s. Doing so greatly reduces the systematic uncertainty from the prompt δ function in all but one set of runs. The presence of an order-of-magnitude larger prompt peak for the $^2P_{1/2}$ transition measured in the linear trap, due to poor optical alignment, results in a significantly larger variation in the fit over the time range and hence the resulting systematic uncertainty for this data set is three times larger than for the other three measurements. Despite this problem, the agreement between the measured $^2P_{3/2}$ lifetimes in both trap apparatuses is nominal, giving us great confidence in our

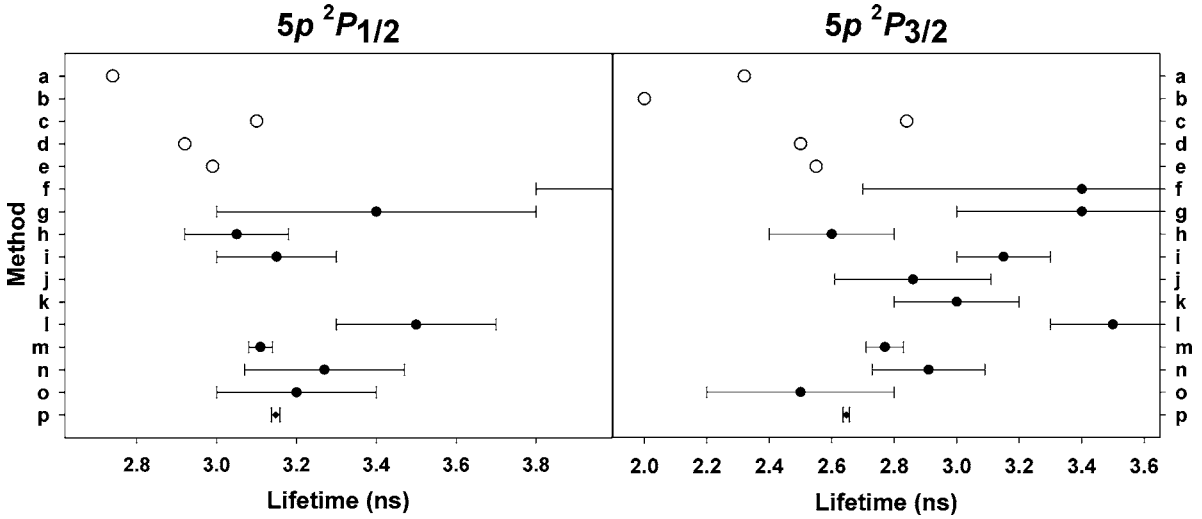

FIG. 3. Published results of theoretical (open circles) and experimental (filled circles) lifetimes, including this work (filled diamonds), for the $5p\ ^2P_{1/2}$ and $5p\ ^2P_{3/2}$ states of Cd^+. (a) Hanle theory (1974) [23], (b) theory (1975) [24], (c) many body perturbation theory (1997) [25], (d) and (e) pseudorelativistic Hartree-Fock theory (2004) [9], (f) phaseshift (1970), $^2P_{1/2}$ value is 4.8 ns [26], (g) beam-foil (1973) [27], (h) Hanle (1974) [23], (i) Electron-photon (1975) [13], (j) Hanle (1976) [28], (k) Hanle (1976) [29], (l) delayed coincidence (1980) [30], (m) beam-laser (1994) [5], (n) beam-foil (1994) [5], (o) laser-induced fluorescence (2004) [9], and (p) this experiment.

technique to account for the much smaller effects of the prompt scattered events in the other three data sets.

The final values, summarized in Table I for each trap, are 3.148 ± 0.011 ns for the $^2P_{1/2}$ state and 2.647 ± 0.010 ns for the $^2P_{3/2}$ state. The final error is the average of the statistical error (less than 0.15% for all measurements) and the systematic error. The systematic error of approximately 0.4% is due to the uncertainty in comparison of the fitted values of the convolved spectrum and the experimental data. These new results are plotted in Fig. 3 along with previously reported theoretical and experimental values for these levels. It is seen that the results reported in this paper are the most precise measurements of these particular excited states of Cd^+.

In conclusion, to our knowledge, we have demonstrated a new technique for measuring excited state atomic lifetimes that is able to eliminate common systematic errors associated with such measurements. The results herein are not only the most precise to date for Cd^+, but with absolute uncertainties of order 10 ps, are among the most precisely measured excited state lifetimes in any atomic system. Furthermore, this technique has the potential to achieve ~ 100 ppm precision by eliminating the remaining systematic effects due to prompt events and electronic noise. Other possible improvements include increasing the data collection rate by using a faster pulse generator and TDC, and measuring a longer decay range by pulse-picking individual pulses.

This work is supported by the U.S. National Security Agency and Advanced Research and Development Activity under Army Research Office contract and the National Science Foundation Information Technology Research Program.

[1] C. S. Wood, S. C. Bennett, D. Cho, B. P. Masterson, J. L. Roberts, C. E. Tanner, and C. E. Wieman, Science **275**, 1759 (1997).
[2] L. J. Curtis, *Atomic Structure and Lifetimes* (Cambridge University Press, Cambridge, 2003).
[3] Z. S. Li, H. Lundberg, G. M. Wahlgren, and C. M. Sikström, Phys. Rev. A **62**, 032505 (2000).
[4] L. Young, W. T. Hill, III, S. J. Sibener, S. D. Price, C. E. Tanner, C. E. Wieman, and S. R. Leone, Phys. Rev. A **50**, 2174 (1994).
[5] E. H. Pinnington, J. J. van Hunen, R. N. Gosselin, B. Guo, and R. W. Berends, Phys. Scr. **49**, 331 (1994).
[6] R. G. DeVoe and R. G. Brewer, Opt. Lett. **19**, 1891 (1994).
[7] R. G. DeVoe and R. G. Brewer, Phys. Rev. Lett. **76**, 2049 (1996).
[8] S. Aubin, E. Gomez, L. A. Orozco, and G. D. Sprouse, Opt. Lett. **28**, 2055 (2003).
[9] H. L. Xu, A. Persson, S. Svanberg, K. Blagoev, G. Malcheva, V. Pentchev, E. Biémont, J. Campos, M. Ortiz, and R. Mayo, Phys. Rev. A **70**, 042508 (2004).
[10] A. Gaupp, P. Kuske, and H. J. Andrä, Phys. Rev. A **26**, 3351 (1982).
[11] R. J. Rafac, C. E. Tanner, A. E. Livingston, and H. G. Berry, Phys. Rev. A **60**, 3648 (1999).
[12] R. E. Imhof and F. H. Read, J. Phys. B **4**, 450 (1971).
[13] D. A. Shaw, A. Adams, and G. C. King, J. Phys. B **8**, 2456 (1975).
[14] J. Lefers, N. Miller, D. Rupke, D. Tong, and M. Walhout, Phys. Rev. A **66**, 012507 (2002).
[15] M. Zinner, P. Spoden, T. Kraemer, G. Birkl, and W. Ertmer, Phys. Rev. A **67**, 010501(R) (2003).
[16] C. W. Oates, K. R. Vogel, and J. L. Hall, Phys. Rev. Lett. **76**, 2866 (1996).
[17] W. I. McAlexander, E. R. I. Abraham, N. W. M. Ritchie, C. J. Williams, H. T. C. Stoof, and R. G. Hulet, Phys. Rev. A **51**, R871 (1995).
[18] E. Peik, G. Hollemann, and H. Walther, Phys. Rev. A **49**, 402 (1994).
[19] S. R. Jefferts, C. Monroe, E. W. Bell, and D. J. Wineland, Phys. Rev. A **51**, 3112 (1995).
[20] It would be possible to increase the data rate by increasing this excitation probability, however, it was kept to near 10% since higher pulsed laser powers also tend to load extra ions into the trap.
[21] D. J. Berkeland, J. D. Miller, J. C. Bergquist, W. M. Itano, and D. J. Wineland, J. Appl. Phys. **83**, 5025 (1998).
[22] Due to the chromatic aberration of this imaging system, the state-selective light collection between $^2P_{1/2}$ and $^2P_{3/2}$ is also achieved.
[23] J. Hamel and J.-P. Barrat, Opt. Commun. **10**, 331 (1974).
[24] M. D. Kunisz, J. Migdałek, and J. Rutkowski, Acta Phys. Pol. A **47**, 227 (1975).
[25] H.-S. Chou and W. R. Johnson, Phys. Rev. A **56**, 2424 (1997).
[26] S. R. Baumann and W. H. Smith, J. Opt. Soc. Am. **60**, 345 (1970).
[27] T. Andersen and G. Sørensen, J. Quant. Spectrosc. Radiat. Transf. **13**, 369 (1973).
[28] F. H. K. Rambow and L. D. Schearer, Phys. Rev. A **14**, 1735 (1976).
[29] T. Andersen, O. Poulsen, and P. S. Ramanujam, J. Quant. Spectrosc. Radiat. Transf. **16**, 521 (1976).
[30] Y. F. Verolainen and V. I. Privalov, Opt. Spectrosc. **48**, 245 (1980).
[31] M. P. Silverman, S. Haroche, and M. Gross, Phys. Rev. A **18**, 1507 (1978).
[32] R. S. Vallery, P. W. Zitzewitz, and D. W. Gidley, Phys. Rev. Lett. **90**, 203402 (2003).